

Supplementary information

Twentieth and Twenty-first Century Water Storage Changes in the Nile River Basin from GRACE/GRACE-FO and Modeling

Emad Hasan^{1,2*}, Aondover Tarhule³, Pierre-Emmanuel Kirstetter^{4,5,6}

¹*Department of Geological Sciences and Environmental Studies, State University of New York, SUNY at Binghamton, Vestal, NY, USA.*

²*Geology Department, Faculty of Science, Damietta University, New Damietta, Egypt.*

³*Department of Geography, Geology, and the Environment, Illinois State University, Normal, IL, USA.*

⁴*School of Meteorology, University of Oklahoma, Norman, OK, USA.*

⁵*School of Civil Engineering and Environmental Science, University of Oklahoma, Norman, OK, USA.*

⁶*NOAA/National Severe Storms Laboratory, Norman, OK, USA.*

To be submitted to the Remote Sensing Journal

***Corresponding Author**

Emad Hasan, Ph.D.

Email: emad.hasan@binghamton.edu

Contents of this file

Figures S1 to S6

Tables S1 to S5

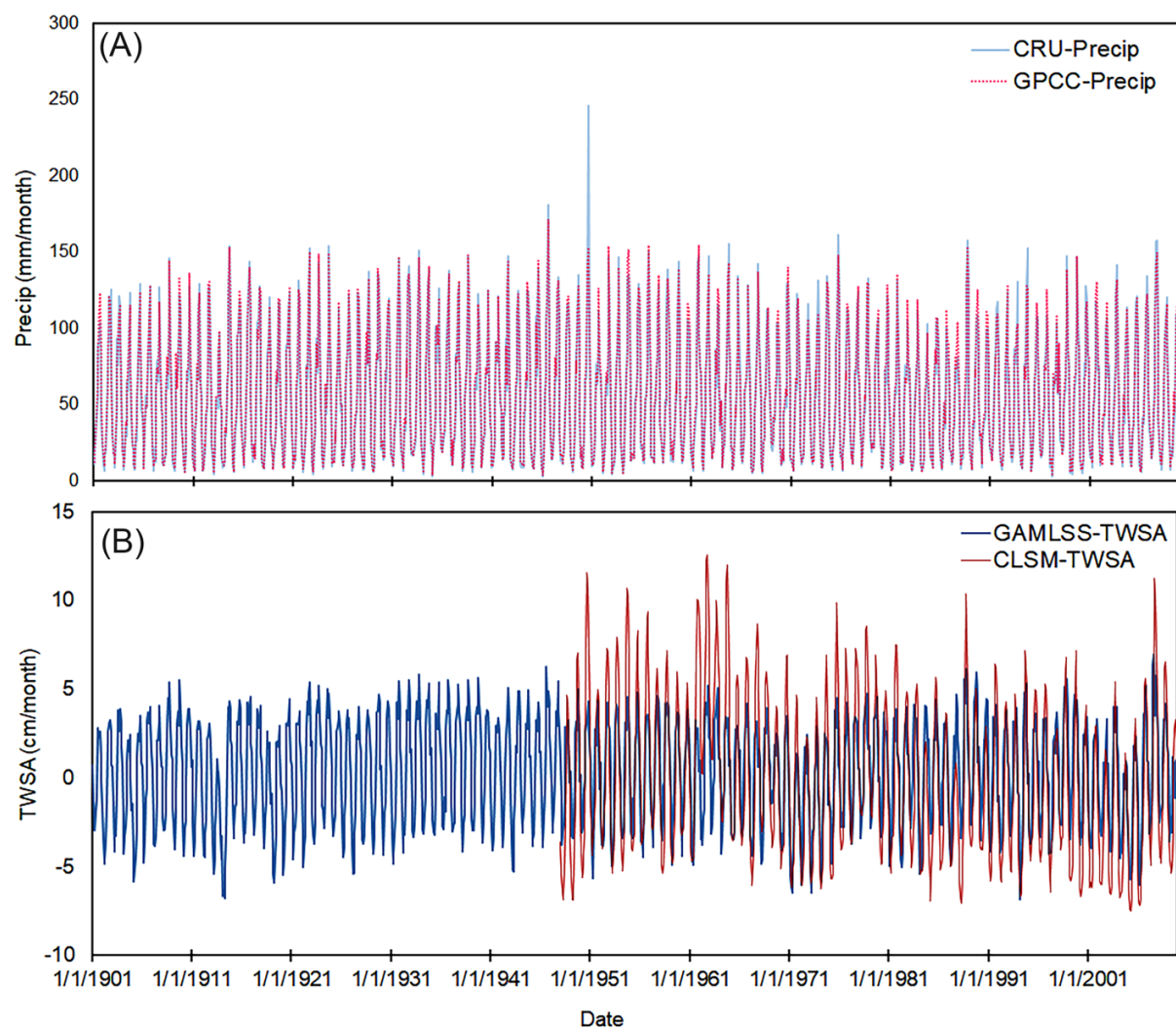


Figure S1. Coevolution between monthly GPCC and CRU precipitation data (A), and GAMLSS-based TWSA and CLMS TWSA (B).

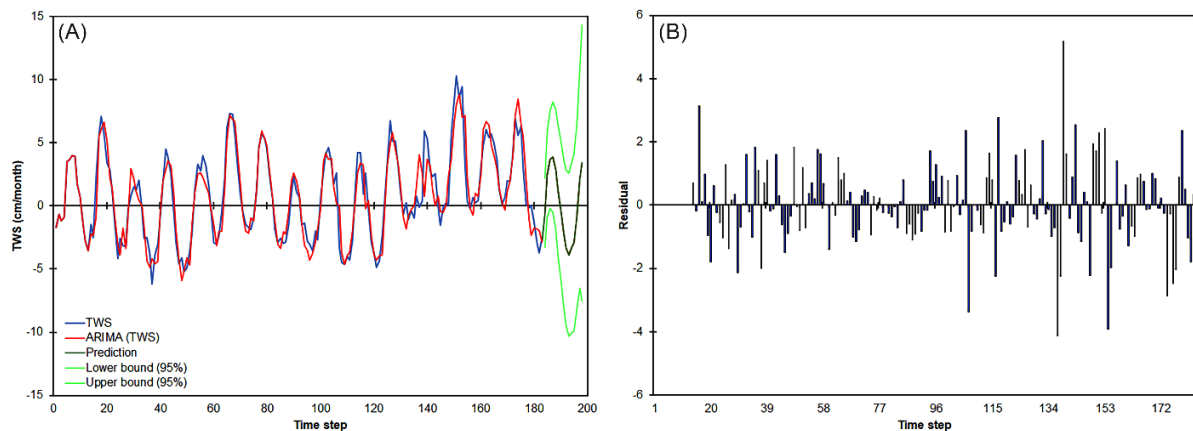


Figure S2. Simulated ARIMA TWS (A), the dark blue of the plot is the one-year gap, plot (B) shows the residual the model.

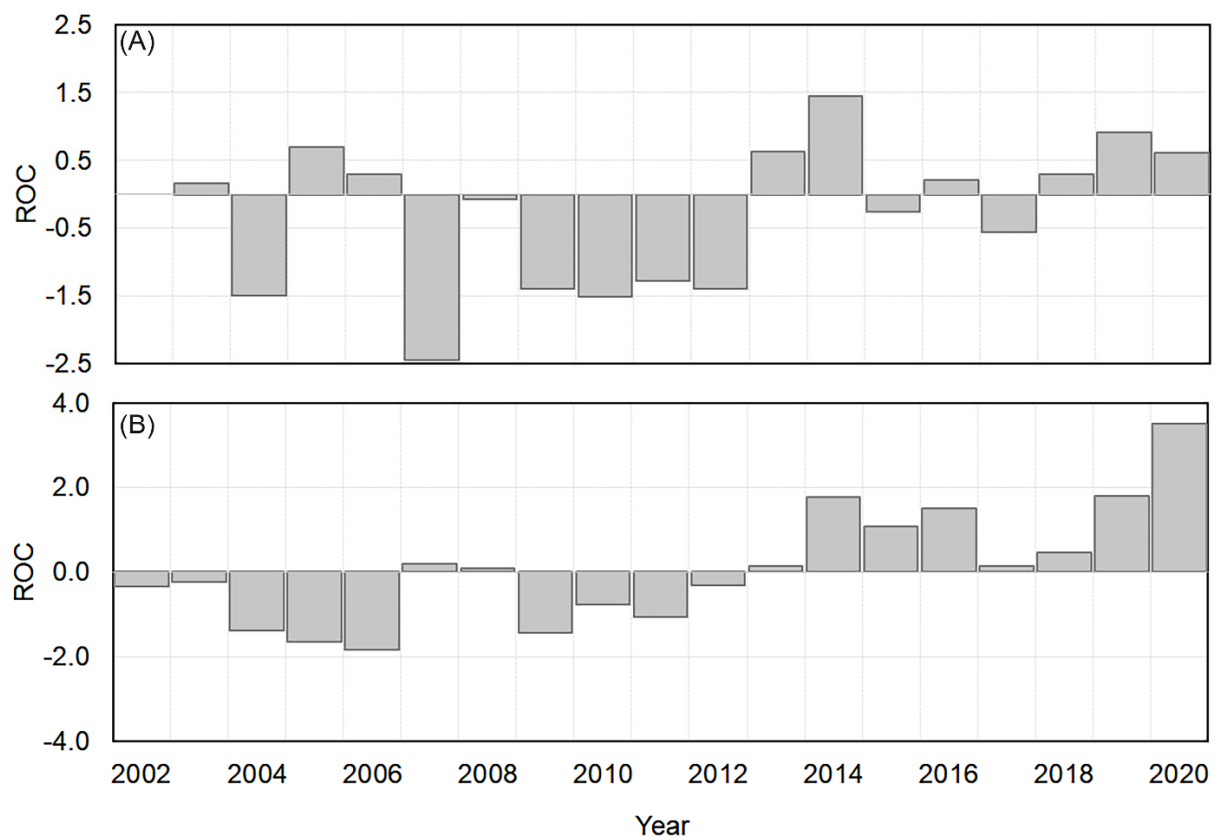


Figure S3. The year-to-year changes in TWSA (A) between 2002 to 2020, and the yearly changes (compared to the overall average) of the TWSA (B) across the NRB.

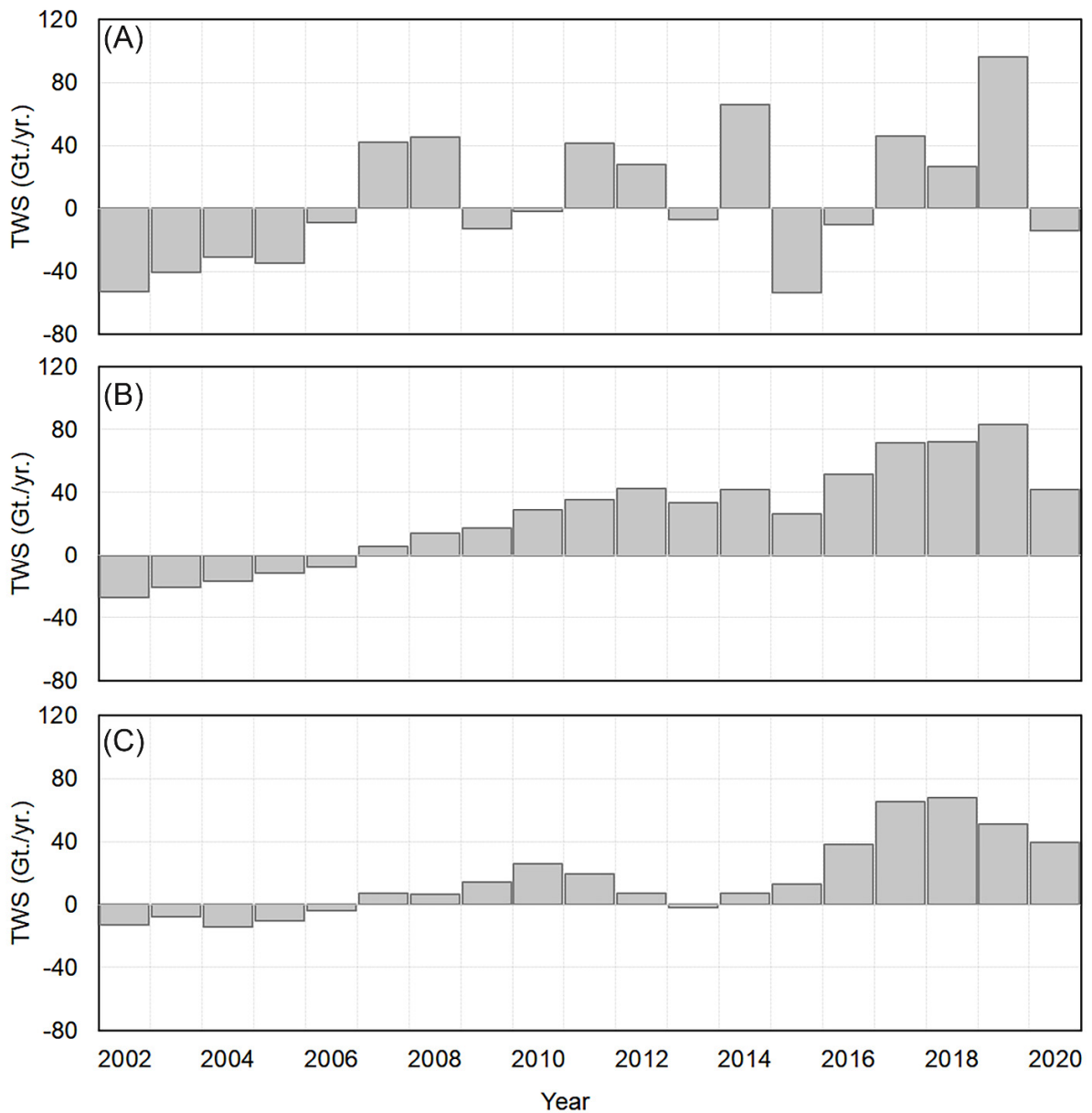


Figure S4. GRACE-based net storage changes between 2002 to 2020 across BNB (A), WNB (B) and Atbara sub-basins (C).

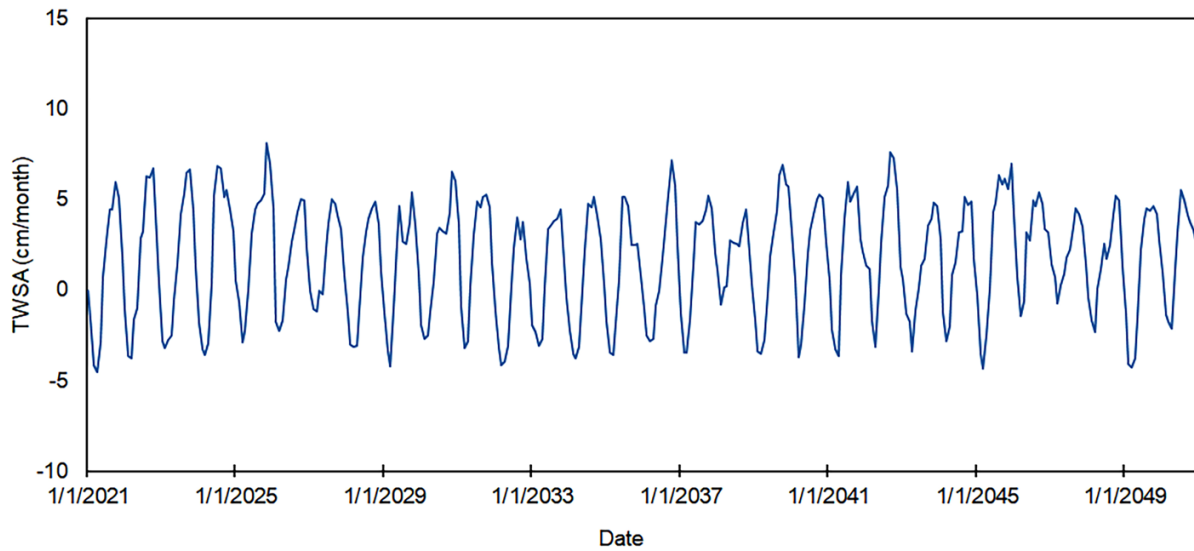


Figure S5. Monthly projected TWSA between 2021 to 2050.

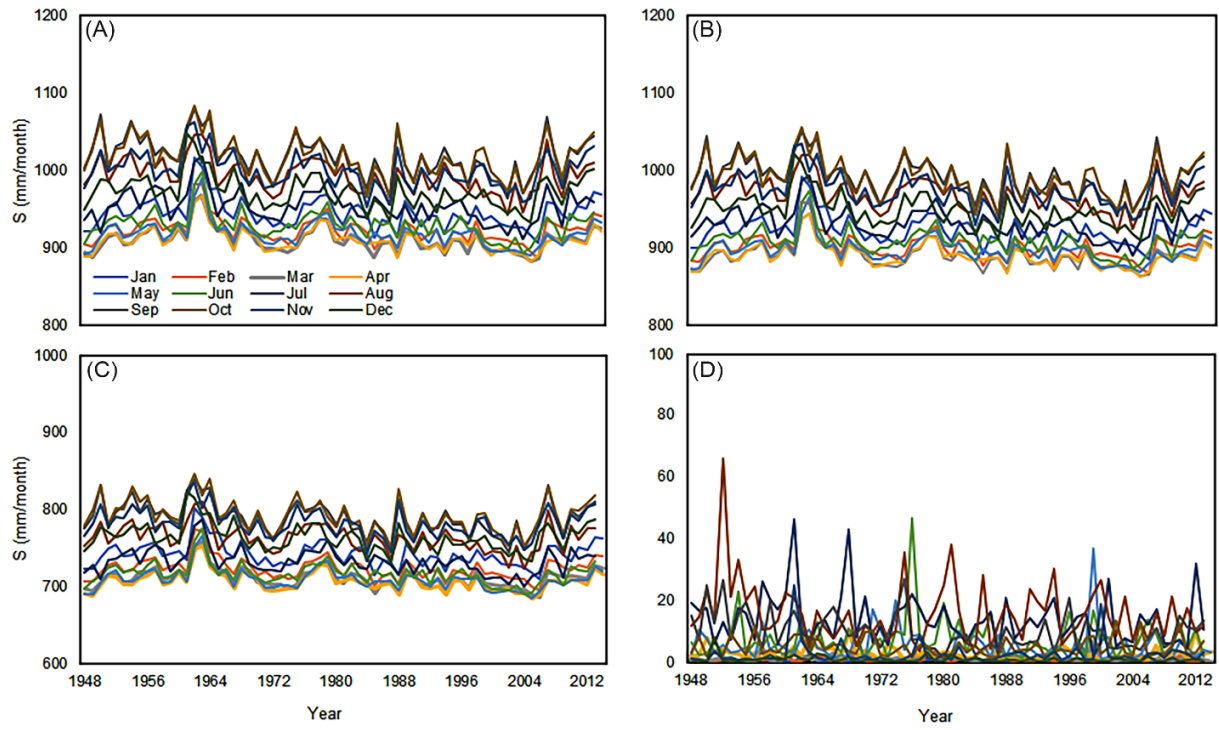


Figure S6. NRB storage figures from TWS (A), GWS (B), SMS (C), and runoff (D)

between 1948 to 2014 from CLSM-F2.5 LSM. The storage-based figures are relatively higher relative to the runoff in the basin.

Table S1. Source information for datasets and drought indicators utilized in this research.

Data	Link	Resolution	Reference
TWS	https://grace.jpl.nasa.gov/data/get-data/	1.0° (SH06)	[1]
		0.25° (M06 CSR)	[2]
		0.5° (M06 JPL)	[3]
LSM-TWS	https://disc.gsfc.nasa.gov/datasets/GLDAS_CL_SM025_D_2.0/summary	0.25°	[4]
Precip.	GPCC, http://gpcc.dwd.de	0.5°	[5]
	CRU, http://www.cru.uea.ac.uk/data	0.5°	[6]
Temp.	CRU, http://www.cru.uea.ac.uk/data	0.5°	[6]
PET	CRU, http://www.cru.uea.ac.uk/data	0.5°	[6]
GPCC_DI	https://www.dwd.de/EN/ourservices/gpcc/gpcc.html	1.0°	[7]
ScPDSI	https://www.rdocumentation.org/packages/scPDSI/versions/0.1.3	0.5°	[8]
SPI	https://digital.csic.es/handle/10261/10006	0.5°	[9]
SPIE	https://digital.csic.es/handle/10261/202305	0.5°	[10]
ClimGen	https://crudata.uea.ac.uk/~timo/climgen/#data	---	[11]

Table S2. GAMLESS (A) and ARIMA (B) models' goodness-of-fit criteria.

(A)	(B)
Paras	AIC
Precipitation	794.36
Temperature	873.46
R ² (GAMLSS)= 0.86	Observations 170
NSCE (GAMLSS)= 0.86	DF 166
R ² (ARIMA)= 0.87	SSE 278.44
NSCE (ARIMA)= 0.87	MSE 1.64
	RMSE 1.28
	WN Variance 1.92
	MAPE(Diff) 90.31
	MAPE 661.75
	-2Log (Like.) 599.03
	FPE 1.64
	AIC 607.02
	AICC 607.27
	BIC 619.57
	Iterations 31

Models' metrics

Residual Sum Squares (RSS) or Sum Squared Error (SSE),

$$RSS = SSE = \sum_{i=1}^n (\varepsilon_i)^2 = \sum_{i=1}^n (y_i - (\alpha + \beta x_i))^2 = \sum_{i=1}^n (y_i - \hat{y}_i)^2 \quad (A1)$$

where, (y_i) is the observed, and (\hat{y}_i) is the modeled parameter using a general linear regression formulation, ($y_i = \alpha + \beta x_i$).

Mean Squared Error (MSE),

$$MSE = \frac{1}{n} \sum_{i=1}^n (y_i - \hat{y}_i)^2 \quad (A2)$$

Correlation Coefficient (R²),

$$R^2 = \frac{\sum (y_i - \hat{y}_i)^2}{\sum (y_i - \bar{y})^2} \quad (A3)$$

Nash-Sutcliffe Coefficient Efficiency,

$$NSCE = 1 - \frac{\sum(\hat{y}_i - y_i)^2}{\sum(y_i - \bar{y})^2} \quad (\text{A4})$$

where, the mean of the squares of errors between the observed (y_i) and the modeled (\hat{y}_i).

Classic Akaike information criterion (Classic AIC),

$$AIC = 2k - 2 \ln(L) \quad (\text{A5})$$

where, (k) is the number of model parameters, (L) is the maximum likelihood.

Akaike information criterion corrected (AICc),

$$AIC_c = \ln \frac{RSS}{n-k} + \frac{n+k}{n-k-2} \quad (\text{A6})$$

Bayesian Information Criterion (BIC),

$$BIC = n \cdot \ln(MSE) + k \cdot \ln(n) \quad (\text{A7})$$

Likelihood Ratio test (LRT), White Noise Variance (WN Variance), Mean Absolute Percentage Error (MAPE), Fit Percentage estimation (FPE).

Table S3. Standard thresholds used to identify the drought and flooding severity levels.

Category	Description	GRACE-DSI & PDSI
W4	Exceptionally Wet	2.0 or greater
W3	Extremely Wet	1.60 to 1.99
W2	Very Wet	1.30 to 1.59
W1	Moderately Wet	0.80 to 1.29
W0	Slightly Wet	0.50 to 0.79
WD	Near Normal	0.49 to -0.49
D0	Abnormally dry	-0.50 to -0.79
D1	Moderate drought	-0.80 to -1.29
D2	Severe drought	-1.30 to -1.59
D3	Extreme drought	-1.60 to -1.99
D4	Exceptional drought	-2.0 or less

Table S4. Summary of the regime-shift analysis of the NRB mean TWS between 2002 to 2020.

TWS (Mean)	Uncert	Length (Month)	Date	
			Begin	End
33.33	± 4.68	22	04/2002	01/2004
-58.27	± 4.16	30	2/2004	01/2009
58.55	± 3.76	30	02/2009	06/2012
-24.76	± 4.55	41	12/2008	06/2012
86.20	± 5.03	85	07/2012	07/2019
280.82	± 5.56	9	08/2019	04/2020

Table S5. Summary of the regime-shift analysis of the NRB in the TWS cyclic component between 2002 to 2020.

TWS (Cycle)	Uncert	Length (Month)	Date	
			Begin	End
45.28	± 2.81	24	04/2002	03/2004
-41.38	± 2.74	31	4/2004	10/2006
36.31	± 3.04	25	11/2006	11/2008
-42.77	± 2.56	43	12/2008	06/2012
5.83	± 3.21	18	07/2012	12/2013
49.31	± 2.89	33	01/2014	09/2016
-35.57	± 3.45	9	10/2016	06/2017
68.65	± 3.36	23	07/2017	05/2019
251.46	± 4.24	11	06/2019	04/2020

Reference

1. Landerer, F., *TELLUS_GRAC_L3_JPL_RL06_LND_v03*. Ver. RL06 v03. PO.DAAC, CA, USA. *Dataset accessed [2020-7-10] at <https://doi.org/10.5067/TELND-3AJ63>.* 2020.
2. Save, H., *CSR GRACE RL06 Mascon Solutions*. *Dataset accessed [2019-09-8]*, H. Save, Editor. 2019, Texas Data Repository Dataverse.
3. Wiese, D.N., et al., *JPL GRACE and GRACE-FO Mascon Ocean, Ice, and Hydrology Equivalent Water Height Coastal Resolution Improvement (CRI) Filtered Release 06 Version 02*. Ver. 02. PO.DAAC, CA, USA. *Dataset accessed [2019-03-11] at <https://doi.org/10.5067/TEMSC-3JC62>.* 2019
4. Li, B., et al., *GLDAS Catchment Land Surface Model L4 daily 0.25 x 0.25 degree V2.0*, Greenbelt, Maryland, USA, Goddard Earth Sciences Data and Information Services Center (GES DISC), Accessed: [7/10/2020], 10.5067/LYHA9088MFWQ. 2018.
5. Schneider, U., et al., *Global Precipitation Analysis Products of the GPCC*. 2011: Deutscher Wetterdienst, Offenbach a. M., Germany.
6. Jones, P.D. and I.C. Harris, *CRU TS3.21: Climatic Research Unit (CRU) Time-Series (TS) Version 3.21 of High Resolution Gridded Data of Month-by-month Variation in Climate (Jan. 1901- Dec. 2012)*. 2013, University of East Anglia Climatic Research Unit: NCAS British Atmospheric Data Centre, 24 September 2013.
7. Finger, P., et al., *GPCC Interpolation Test Dataset at 1.0°*. 2015, Global Precipitation Climatology Centre (GPCC) at Deutscher Wetterdienst.
8. Zhong, R., et al., *scPDSI: Calculation of the Conventional and Self-Calibrating Palmer Drought Severity Index*. 2018.
9. Beguería, S. and S. Vicente, *SPI Calculator*. 2009.
10. Beguería, S. and S. Vicente, *SPElbase v.2.6 [Dataset]*. 2020.
11. Osborn, T.J., *A user guide for ClimGen: a flexible tool for generating monthly climate data sets and scenarios*, in *ClimGen version 1-02*. 2009, Climatic Research Unit (CRU): School of Environmental Sciences, University of East Anglia, Norwich NR4 7TJ, UK. p. 1-17.